Available online at www.sciencedirect.com

SciVerse ScienceDirect

Ceramics International 39 (2013) 2781–2786

CERAMICS INTERNATIONAL

www.elsevier.com/locate/ceramint

Synthesis and negative thermal expansion property of $Y_{2-x}La_xW_3O_{12}$ ($0 \le x \le 2$)

Hongfei Liu[a,*], Zhiping Zhang[b], Wei Zhang[a], Xianghua Zeng[a], Xiaobing Chen[a]

[a]School of Physics Science and Technology, Yang zhou University, Yang zhou 225009, PR China
[b]Department of Electrical and Mechanical Engineering, Jianghai College, Yang zhou 225009, PR China

Received 17 July 2012; received in revised form 11 September 2012; accepted 12 September 2012
Available online 19 September 2012

Abstract

$Y_{2-x}La_xW_3O_{12}$ solid solutions were successfully synthesized by the solid state reaction method. The microstructure, hygroscopicity and thermal expansion property of the resulting samples were investigated by X-ray diffraction (XRD), thermogravimetric analysis (TGA), field emission scanning electron microscopy (FESEM) and thermal mechanical analysis (TMA). Results indicate that the structural phase transition of the $Y_{2-x}La_xW_3O_{12}$ changes from orthorhombic to monoclinic with increasing substituted content of lanthanum. The pure phase can form for $0 \le x \le 0.4$ with orthorhombic structure and for $1.5 \le x \le 2$ with monoclinic one. High lanthanum content leads to a low relative density of $Y_{2-x}La_xW_3O_{12}$ ceramic. Thermal expansion coefficients of the $Y_{2-x}La_xW_3O_{12}$ ($0 \le x \le 2$) ceramics also vary from $-9.59 \times 10^{-6}\,K^{-1}$ to $2.06 \times 10^{-6}\,K^{-1}$ with increasing substituted content of lanthanum. The obtained $Y_{0.25}La_{1.75}W_3O_{12}$ ceramic shows almost zero thermal expansion and its average linear thermal expansion coefficient is $-0.66 \times 10^{-6}\,K^{-1}$ from 103 °C to 700 °C.

Keywords: B. Composites; C. Thermal expansion; D. Ceramics ; Tungstates

1. Introduction

Thermal expansion is generally considered to be an important property in the application of highly functional materials because the mismatch of thermal expansion between component materials can cause problems, such as mechanical destruction and positional deviation, in electrical, optical and high-temperature devices. One of the possible methods that can solve these problems is preparing materials with controllable or near-zero expansion coefficient. Recently, negative thermal expansion (NTE) materials have attracted widespread interests due to their potential applications in controllable thermal expansion composites and coatings. We can combine the negative thermal expansion materials with positive thermal expansion materials to form various materials with controllable thermal expansion, being positive, negative or even zero.

Much attention has been recently paid to the materials with the general formula $A_2W_3O_{12}$ owing to their interesting physical and chemical properties. It has been found that there are two structures in the family of $A_2W_3O_{12}$ compounds, orthorhombic and monoclinic, and the thermal expansion property is mainly related to the exact structure of the compound [1]. Compounds with orthorhombic structures exhibit negative thermal expansion, such as $Sc_2W_3O_{12}$ [3,4], $Y_2W_3O_{12}$ [1,5,6], $Er_2W_3O_{12}$ [1,7] and $Lu_2W_3O_{12}$ [8], this orthorhombic structure is composed of corner-shared AO_6 octahedra and WO_4 tetrahedra. A–O–W linkages in their structures can accommodate transverse thermal vibrations and lead to the NTE [6]. Compounds with monoclinic structures exhibit positive thermal expansion, such as $La_2W_3O_{12}$ [1,2], $Dy_2W_3O_{12}$ [1], and $Nd_2W_3O_{12}$ [1], this monoclinic structure is composed of edge-sharing AO_8 polyhedra and WO_4 tetrahedra.

It is reported that controllable thermal expansion coefficient in $A_2W_3O_{12}$ may be obtained by partial chemical substitution of the A cation by another trivalent cation [9–13]. $Y_2W_3O_{12}$ crystallizes in an orthorhombic symmetry

*Corresponding author. Tel.: +86 514 87975466; fax: +86 514 87975467.
E-mail address: liuhf@yzu.edu.cn (H. Liu).

0272-8842/$ - see front matter © 2012 Elsevier Ltd and Techna Group S.r.l. All rights reserved.
http://dx.doi.org/10.1016/j.ceramint.2012.09.045

(*Pnca*) and exhibits NTE with the linear thermal expansion coefficient of $-8.35\times10^{-6}\,K^{-1}$ in the temperature range from 300 K to 1100 K [14]. However, $La_2W_3O_{12}$ crystallizes in a monoclinic symmetry (*C*2/*c*) and exhibits positive thermal expansion with the linear thermal expansion coefficient of $4.14\times10^{-6}\,K^{-1}$ in the temperature range from room temperature to 1073 K [1]. It is therefore possible to obtain the $Y_{2-x}La_xW_3O_{12}$ ceramic with controllable thermal expansion coefficient by partial substitution of Y^{3+} with La^{3+}, and control the thermal expansion coefficient to be negative, positive and even zero by careful adjustment of the Y/La ratio. Here in this report, a new series of $Y_{2-x}La_xW_3O_{12}$ ($0\le x\le2$) ceramics was successfully prepared by the solid state reaction method and the effects of substituted lanthanum content on the microstructure, density, hygroscopicity and thermal expansion property were also studied.

2. Experimental

2.1. Preparation of the $Y_{2-x}La_xW_3O_{12}$ ($0\le x\le2$) samples

The samples of $Y_{2-x}La_xW_3O_{12}$ ($0\le x\le2$) ceramics were prepared by the conventional solid state reaction method. Starting materials were Y_2O_3 (purity ≥ 99.9%), La_2O_3 (purity ≥ 99.5%) and WO_3 (purity ≥ 99.5%). All the starting materials were pre heated at 300 °C for 24 h before weighting to protect from H_2O. Stoichiometric ratios of the reactants were milled for 10 h to form a uniform mixture and dried at 90 °C, and then the mixtures were pre-calcined at 600 °C for 10 h. After pre-sintering, the mixtures were pressed into pellets (10 mm diameter and 2.5 mm height), and finally calcined at 1050 °C in air for 10 h.

2.2. Experimental techniques

The resulting samples were characterized by powder X-ray diffraction (XRD) using Cu Kα radiation ($\lambda=0.15418$ nm) with 40 kV/20 mA (D/max2500, Rigaku). The XRD data were collected with a scanning speed of 5° (2θ) per minute in the 2θ range from 10° to 50° by the continuum scanning method. The thermogravimetric curves of the samples were collected in the open air from room temperature to 300 °C using thermogravimetric analysis (TGA, Pyris1). The heating rate was 10 °C/ min. The microstructures of the samples were observed by a field emission scanning electron microscopy (FESEM, Hitachi S-4800) under an acceleration voltage of 15 kV. Densities of the samples were measured using Archimedes' method. The thermal expansion coefficients of the samples were measured by thermal mechanical analyzer (TMA/SS, Seiko 6300). The measurements were carried out at the rate of 10 °C/min in the open air from room temperature to 700 °C.

3. Results and discussion

3.1. XRD analysis

Fig. 1 shows the typical XRD patterns of the obtained $Y_{2-x}La_xW_3O_{12}$ ($x=0$, 0.4, 0.5, 1, 1.5, 1.75, and 2) samples. As one can see in Fig. 1(e), (f) and (g), the $Y_{2-x}La_xW_3O_{12}$ ($x=1.5$, 1.75, and 2) samples, synthesized with different amount of lanthanum, have almost the same XRD patterns, and all the peak positions of these samples are well indexed to the $La_2W_3O_{12}$ (JCPDS 15-0438), indicating pure phase of $Y_{2-x}La_xW_3O_{12}$ can form for $1.5\le x\le2$ with monoclinic $La_2W_3O_{12}$-type structure. However, the samples $Y_{2-x}La_xW_3O_{12}$ ($0.4<x<1.5$) are isolated as biphasic mixture, and they contain both monoclinic and orthorhombic phases, and some representative reflections of the two phases are labeled in Fig. 1(c) and (d). $Y_{2-x}La_xW_3O_{12}$ can also form pure phase for $0\le x\le0.4$ with orthorhombic $Y_2W_3O_{12}$–type structure. The XRD patterns of the $Y_{2-x}La_xW_3O_{12}$ ($x=0$, 0.4, 0.5) are similar to those reported for $Y_2W_3O_{12}\cdot nH_2O$, which is hygroscopic at room temperature [1,5,6,14]. The board humps in the XRD patterns indicate that some amorphous phase might form owing to the absorption of water molecules in the frame-structure.

Compared with the XRD patterns of the $Y_{2-x}La_xW_3O_{12}$ ($x=1.5$, 1.75, and 2), it is found that all the diffraction lines shift toward lower 2θ angles with the increase of lanthanum content, which can be obviously seen in Fig. 2. It indicates that the lattice parameters of $Y_{2-x}La_xW_3O_{12}$ ($x=1.5$, 1.75, 2) increase with increasing lanthanum content owing to that the ionic radii of La^{3+} (106.1 pm) is larger than that of Y^{3+} (90 pm). This is in good agreement with the Vegard's law, and on the other hand it proves that the $Y_{2-x}La_xW_3O_{12}$ ($1.5\le x\le2$) compounds have been successfully synthesized.

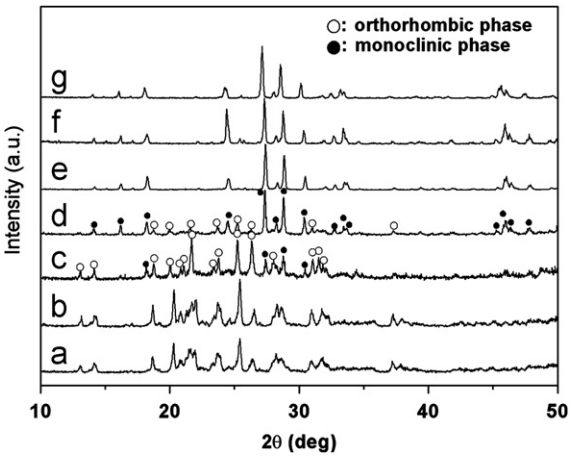

Fig. 1. XRD patterns of the obtained $Y_{2-x}La_xW_3O_{12}$ ($x=0$, 0.4, 0.5, 1, 1.5, 1.75, and 2) ceramics (a) $Y_2W_3O_{12}$, (b) $Y_{1.6}La_{0.4}W_3O_{12}$, (c) $Y_{1.5}La_{0.5}W_3O_{12}$, (d) $Y_1La_1W_3O_{12}$, (e) $Y_{0.5}La_{1.5}W_3O_{12}$, (f) $Y_{0.25}La_{1.75}W_3O_{12}$, and (g) $La_2W_3O_{12}$.

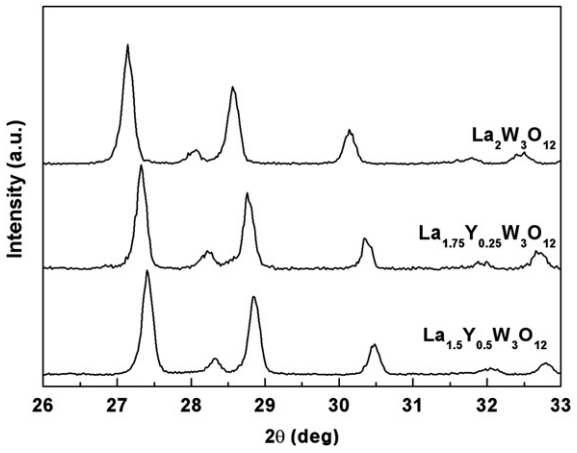

Fig. 2. XRD patterns of the obtained $Y_{2-x}La_xW_3O_{12}$ (x=1.5, 1.75, and 2) ceramics.

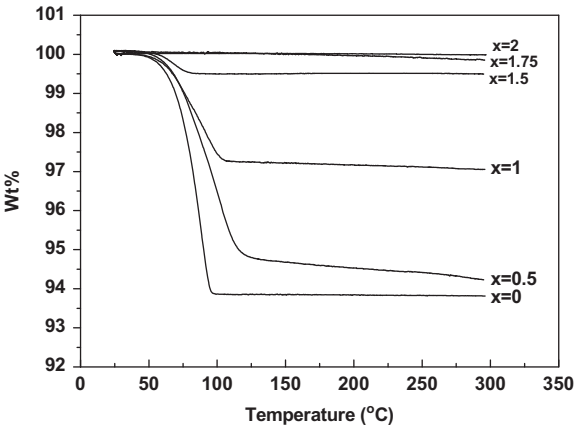

Fig. 3. Thermogravimetric curves of the obtained $Y_{2-x}La_xW_3O_{12}$ samples (x=0, 0.5, 1, 1.5, 1.75, and 2).

3.2. Thermogravimetric analysis

Fig. 3 shows the thermogravimetric (TG) curves of the obtained $Y_{2-x}La_xW_3O_{12}$ (x=0, 0.5, 1, 1.5, 1.75, and 2) samples; it can be found that there is a mass loss region from 50 °C to 150 °C in the TG curve of the $Y_{2-x}La_xW_3O_{12}$ (x=0, 0.5, 1, and 1.5) samples, indicating the $Y_{2-x}La_xW_3O_{12}$ (x=0, 0.5, 1, and 1.5) is hygroscopic at room temperature, and the mass losses are about 6.17%, 5.23%, 2.71% and 0.58%,. The corresponding numbers of water molecules per formula unit are calculated to be 3.36, 2.90, 1.50 and 0.32. This hygroscopic phenomenon also has been found in some other orthorhombic $A_2W_3O_{12}$ (A=Er, Lu and Y) [1–8]. However, there is no obvious inclination observed from 50 °C to 150 °C in the TG curves of the $Y_{0.25}La_{1.75}W_3O_{12}$ and $La_2W_3O_{12}$, indicating no water of adsorbed moisture in the samples.

3.3. SEM images and density analysis

The SEM fractographs of the obtained $Y_{2-x}La_xW_3O_{12}$ (x=0, 0.5, 1, 1.5, 1.75, and 2) ceramics are shown in Fig. 4. Interestingly, the $Y_{2-x}La_xW_3O_{12}$ (x=0, 0.5, 1, 1.5, 1.75, and 2) ceramics with different x values have different morphologies. In Fig. 4(a), it can be seen that the microstructure of the $La_2W_3O_{12}$ ceramic consists of small grains and lots of pores inside. Compared with the $La_2W_3O_{12}$ ceramic, the $Y_{0.25}La_{1.75}W_3O_{12}$ and $Y_{0.5}La_{1.5}W_3O_{12}$ ceramics contain larger grains and some microcracks; meanwhile, the porosity decrease. With the decrease of the amount of lanthanum ions, the $Y_1La_1W_3O_{12}$, $Y_{1.5}La_{0.5}W_3O_{12}$ and $Y_2W_3O_{12}$ samples become denser, and the pores almost disappear. However, there are still some microcracks that existed in the $Y_1La_1W_3O_{12}$ and $Y_{1.5}La_{0.5}W_3O_{12}$ ceramics, and it has probably caused the large grain size and anisotropy in grain shape. According to the SEM results discussed above, it can be concluded that the microstructures and densities of the $Y_{2-x}La_xW_3O_{12}$ ($0 \le x \le 2$) are affected by the lanthanum content. The densities of the $Y_{2-x}La_xW_3O_{12}$ (x=0, 0.5, 1, 1.5, 1.75, 2) ceramics become denser as the substituted content of lanthanum decreases.

To further investigate the densities of the resulting $Y_{2-x}La_xW_3O_{12}$ (x=0, 0.5, 1, 1.5, 1.75, and 2) ceramics, the densities of the samples were measured using Archimedes' method [15] and the theoretical densities were calculated from theoretical values for $La_2W_3O_{12}$ (6.63 g/cm^3) and $Y_2W_3O_{12}$ (4.36 g/cm^3). The testing results are in good accordance with the SEM analysis above, as shown in Fig. 5. It can be found that the densities of the $Y_{2-x}La_xW_3O_{12}$ (x=0, 0.5, 1, 1.5, 1.75, and 2) ceramics increase with the increasing content of lanthanum. However, the relative densities decrease, and this means the resulting ceramics become loosened. The testing density of $La_2W_3O_{12}$ is 5.23 g/cm^3, which reaches 78.91% of the theoretical density values. Compared with $La_2W_3O_{12}$ ceramics, the relative densities of the $Y_{2-x}La_xW_3O_{12}$ (x=1.75, 1.5, 1, 0.5, and 0) ceramics can reach 82.01%, 87.22%, 91.81%, 93.27% and 95.04% of the theoretical values, respectively.

3.4. Thermal expansion properties

The thermal expansion curves of the obtained $Y_{2-x}La_xW_3O_{12}$ (x=0, 0.5, 1, 1.5, 1.75, and 2) ceramics are shown in Fig. 6. It can be seen that the thermal expansion curves of the $Y_{2-x}La_xW_3O_{12}$ (x=0, 0.5, 1, and 1.5) ceramics all show an initial expansion from room temperature to 200 °C due to the removal of the water molecules (see Fig. 6(a)–(d)), which is also supported by the above thermogravimetric analysis. The general features of these materials in the thermal expansion behaviors are similar to the thermal expansion of the bulk $Y_2W_3O_{12}$ reported [1]. It is reported that water molecules would occupy the crystallographic voids in hydrated $A_2W_3O_{12}$ structure, and the A–O–W linkages bend away from 180° because the water molecules enter the compound. The incorporation of water in the framework structure will hinder the transverse vibrations of A–O–W linkages and prevent negative thermal expansion [14]. The negative thermal expansion will occur after the complete removal of water,

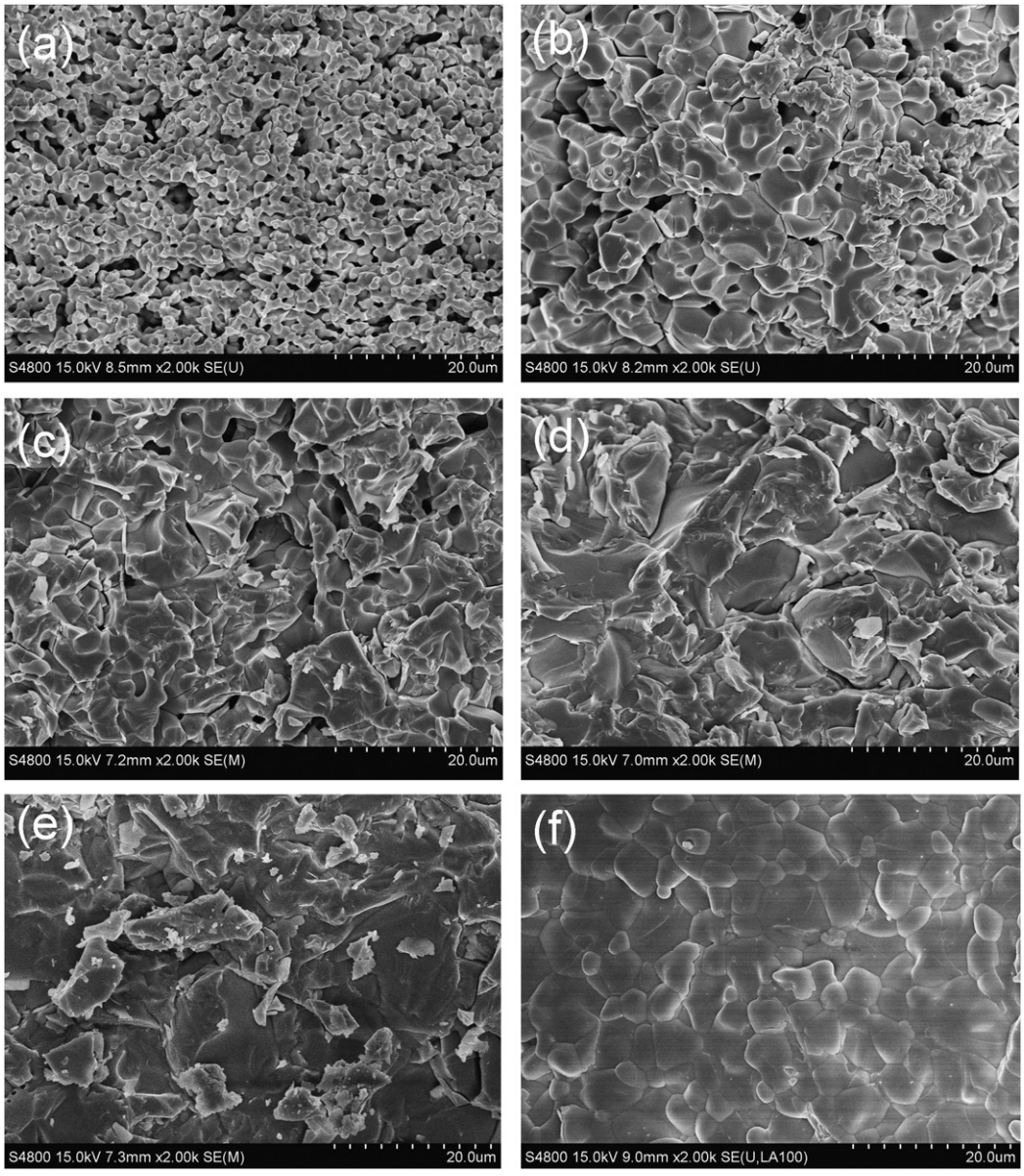

Fig. 4. SEM images of the obtained $Y_{2-x}La_xW_3O_{12}$ ($x=0$, 0.5, 1, 1.5, 1.75, and 2) ceramics (a) $La_2W_3O_{12}$, (b) $Y_{0.5}La_{1.5}W_3O_{12}$, (c) $Y_1La_1W_3O_{12}$, (d) $Y_{1.5}La_{0.5}W_3O_{12}$, (e) $Y_{1.75}La_{0.25}W_3O_{12}$, (f) $Y_2W_3O_{12}$.

and this phenomena can be obviously observed in the thermal expansion curves of the $Y_{2-x}La_xW_3O_{12}$ ($x=0$, 0.5, 1, and 1.5) ceramics. The $Y_{2-x}La_xW_3O_{12}$ ($x=0$, 0.5, 1, and 1.5) ceramics show negative thermal expansion above 200 °C, and Table 1 shows the average linear thermal expansion coefficients of the $Y_{2-x}La_xW_3O_{12}$ ($x=0$, 0.5, 1, 1.5, 1.75, 2) in the corresponding temperature range. The average linear thermal expansion coefficients of the $Y_{2-x}La_xW_3O_{12}$ ($x=0$, 0.5, 1, and 1.5) ceramics are measured to be $-9.59\times10^{-6}\,K^{-1}$, $-8.75\times10^{-6}\,K^{-1}$, $-7.63\times10^{-6}\,K^{-1}$ and $-1.91\times10^{-6}\,K^{-1}$, respectively. Based on the above thermogravimetric analysis, there is no water of adsorbed moisture in the $Y_{0.25}La_{1.75}W_3O_{12}$ sample. Compared with the $Y_{2-x}La_xW_3O_{12}$ ($x\leq1.5$) ceramics, there is almost no thermal expansion hysteresis observed in its thermal expansion curve shown in Fig. 6(e). The average linear thermal expansion coefficient of the $Y_{0.25}La_{1.75}W_3O_{12}$ is measured to be $-0.66\times10^{-6}\,K^{-1}$. This non-hygroscopic and near-zero thermal expansion material $Y_{0.25}La_{1.75}W_3O_{12}$ will have a variety of applications. As shown in Fig. 6(f), the non-hygroscopic monoclinic $La_2W_3O_{12}$ ceramic show positive thermal expansion and the average linear thermal expansion coefficient is measured to be $2.06\times10^{-6}\,K^{-1}$ in the temperature range from 25 °C to 700 °C.

As seen from Table 1, it can be found that the average linear thermal expansion coefficients of the $Y_{2-x}La_xW_3O_{12}$ ($x=0$, 0.5, 1, 1.5, 1.75, and 2) become more negative with the decrease of the content of lanthanum. We can interpret that the Y(La)O_6 octahedra become larger with the

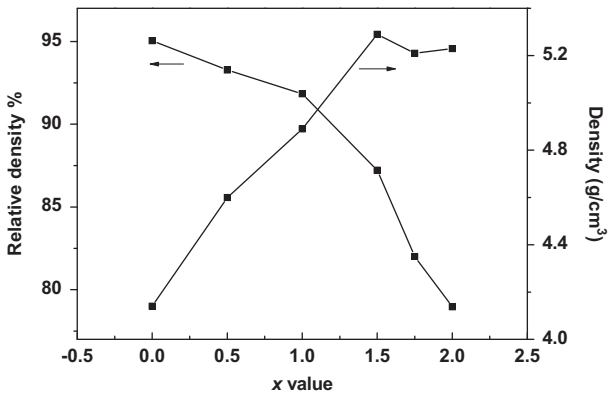

Fig. 5. The density of the obtained $Y_{2-x}La_xW_3O_{12}$ (x=0, 0.5, 1, 1.5, 1.75, and 2) ceramics.

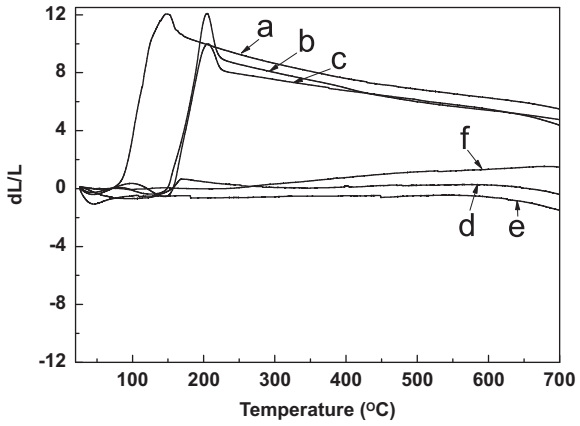

Fig. 6. Thermal expansion curves of the obtained $Y_{2-x}La_xW_3O_{12}$ (x=0, 0.5, 1, 1.5, 1.75, and 2) ceramics.

Table 1
Average linear thermal expansion coefficients of the $Y_{2-x}La_xW_3O_{12}$ (x=0, 0.5, 1, 1.5, 1.75, and 2) ceramics.

$Y_{2-x}La_xW_3O_{12}$	Temperature range (°C)	$\alpha_l(\times 10^{-6}\,K^{-1})$
x=2	25–700	2.06
x=1.75	103–700	−0.66
x=1.5	165–700	−1.96
x=1	232–700	−7.63
x=0.5	230–700	−8.75
x=0	171–700	−9.59

decreasing lanthanum content, and the oxygen–oxygen repulsion in polyhedra decrease. These factors make it easier for polyhedra to experience slight distortions, and the thermal expansion coefficient gets more negative [13]. In this experiment, it can be obviously found that the thermal expansion coefficient of $Y_{2-x}La_xW_3O_{12}$ ceramic can be easily controlled by adjusting the ratio of yttrium and lanthanum.

4. Conclusions

A series of $Y_{2-x}La_xW_3O_{12}$ ($0 \le x \le 2$) solid solutions was synthesized successfully by the solid state reaction method. Pure phase of $Y_{2-x}La_xW_3O_{12}$ can form for $0 \le x \le 0.4$ with orthorhombic structure and $1.5 \le x \le 2$ with monoclinic one. TG analysis shows that $Y_{2-x}La_xW_3O_{12}$ ($0 \le x < 1.75$) are hygroscopic at room temperature and lose water in the temperature range from 50 °C to 150 °C. However, no hygroscopic phenomenon has been observed in the $Y_{2-x}La_xW_3O_{12}$ ($1.75 \le x \le 2$). With the increase of the substituted content of lanthanum, the relative density of the $Y_{2-x}La_xW_3O_{12}$ ceramics decrease, and the average linear negative thermal expansion coefficients of $Y_{2-x}La_xW_3O_{12}$ increase from $-9.59\times10^{-6}\,K^{-1}$ to $2.06\times10^{-6}\,K^{-1}$. We can adjust the thermal expansion coefficients of $Y_{2-x}La_xW_3O_{12}$ ceramics by controlling the substitution ratio of yttrium and lanthanum. The obtained $Y_{0.25}La_{1.75}W_3O_{12}$ ceramic almost exhibits zero thermal expansion and its average linear thermal expansion coefficient is $-0.66\times10^{-6}\,K^{-1}$.

Acknowledgments

The authors thank the National Natural Science Foundation of China (no. 51102207), Yangzhou University Development Foundation for Talents (no.0274640015427) and Yangzhou University Science and Technique Innovation Foundation (no.2010CXJ081).

References

[1] S. Sumithra, A.M. Umarji, Role of crystal structure in the bulk thermal expansion of $Ln_2W_3O_{12}$ (Ln=La, Nd, Dy, Y, Er, Yb), Solid State Sciences 6 (2004) 1313–1319.
[2] H.F. Liu, W. Zhang, Z.P. Zhang, X.B. Chen, Synthesis and negative thermal expansion properties of solid solutions $Yb_{2-x}La_xW_3O_{12}$ ($0 \le x \le 2$), Ceramics International 38 (2012) 2951–2956.
[3] J.S.O. Evans, T.A. Mary, A.W. Sleight, Negative thermal expansion in $Sc_2(WO_4)_3$, Journal of Solid State Chemistry 137 (1998) 148–160.
[4] Q.Q. Liu, J. Yang, X.N. Cheng, G.S. Liang, X.J. Sun, Preparation and characterization of negative thermal expansion $Sc_2W_3O_{12}$/Cu core–shell composite, Ceramics International 38 (2012) 541–545.
[5] D.A. Woodcock, P. Lightfoot, C. Ritter, Negative thermal expansion in $Y_2(WO_4)_3$, Journal of Solid State Chemistry 149 (2000) 92–98.
[6] P.M. Forster, A.W. Sleight, Negative thermal expansion in $Y_2W_3O_{12}$, International Journal Of Inorganic Materials 1 (1999) 123–127.
[7] S. Sumithra, A.K. Tyagi, A.M. Umarji, Negative thermal expansion in $Er_2W_3O_{12}$ and $Yb_2W_3O_{12}$ by high temperature X-ray diffraction, Materials Science and Engineering B 116 (2005) 14–18.
[8] P.M. Forster, A. Yokochi, A.W. Sleight, Enhanced negative thermal expansion in $Lu_2W_3O_{12}$, Journal of Solid State Chemistry 140 (1998) 157–158.
[9] X.L. Xiao, J. Peng, M.M. Wu, Y.Z. Cheng, D.F. Chen, Z.B. Hu, The crystal structure and thermal expansion properties of solid solutions $Ln_{2-x}Dy_xW_3O_{12}$ (Ln=Er and Y), Journal of Alloys and Compounds 465 (2008) 556–561.
[10] J. Peng, M.M. Wu, H. Wang, Y.M. Hao, Z. Hu, Z.X. Yu, D.F. Chen, R. Kiyanagi, J.S. Fieramosca, S. Short, J. Jorhensen, Structures and negative thermal expansion properties of solid

solutions $Y_xNd_{2-x}W_3O_{12}$ (x=0.0–1.0, 1.6–2.0), Journal of Alloys and Compounds 453 (2008) 49–54.

[11] M. Ari, P.M. Jardim, B.A. Marinkovic, F. Rizzo, F.F. Ferreira, Thermal expansion of $Cr_{2x}Fe_{2-2x}Mo_3O_{12}$, $Al_{2x}Fe_{2-2x}Mo_3O_{12}$ and $Al_{2x}Cr_{2-2x}Mo_3O_{12}$ solid solutions, Journal of Solid State Chemistry 181 (2008) 1472–1479.

[12] M.M. Wu, J. Peng, Y.Z. Cheng, X.L. Xiao, Y.M. Hao, Z.B. Hu, Thermal expansion in solid solution $Er_{2-x}Sm_xW_3O_{12}$, Materials Science and Engineering B 137 (2007) 144–148.

[13] M.M. Wu, Y.Z. Cheng, J. Peng, X.L. Xiao, D.F. Chen, R. Kiyanagi, J.S. Fieramosca, S. Short, J. Jorgensen, Z.B. Hu, Synthesis of solid solution $Er_{2-x}Ce_xW_3O_{12}$ and studies of their thermal expansion behavior, Materials Research Bulletin 42 (2007) 2090–2098.

[14] S. Sumithra, A.M. Umarji, Hygroscopicity and bulk thermal expansion in $Y_2W_3O_{12}$, Materials Research Bulletin 40 (2005) 167–176.

[15] X.B. Yang, X.N. Cheng, X.H. Yan, J. Yang, T.B. Fu, J. Qiu, Synthesis of ZrO_2/ZrW_2O_8 composites with low thermal expansion, Composites Science and Technology 67 (2007) 1167–1171.